Loss of genome maintenance accelerates podocyte damage

Fabian Braun[1,2*], Amrei M. Mandel[1,3,4], Linda Blomberg[1,3], Milagros N. Wong[2], Georgia Chatzinikolaou[5], Viji Nair[6], Roman Akbar-Haase[1,3], Victor G. Puelles[2], Phillip J. McCown[6], Fabian Haas[2], Mahdieh Rahmatollahi[1,3], Damian Fermin[8], Gisela G. Slaats[1,3], Tillmann Bork[9], Christoph Schell[9,10], Sybille Koehler[1,2], Paul T. Brinkoetter[1,3], Maja T. Lindenmeyer[2], Clemens D. Cohen[2,11], Martin Kann[1,3], Wilhelm Bloch[12], Matthew G. Sampson[13,14,15], Martijn ET Dollé[16], Matthias Kretzler[6], George A. Garinis[5,17], Tobias B. Huber[2], Bernhard Schermer[1,3,18], Thomas Benzing[1,3,18], Björn Schumacher[3,17,19], and Christine E. Kurschat[1,3*]

[1]Department II of Internal Medicine and Center for Molecular Medicine Cologne, University of Cologne, Faculty of Medicine and University Hospital Cologne, Cologne, Germany
[2]III. Department of Medicine, University Medical Center Hamburg-Eppendorf, Hamburg, Germany
[3]Cologne Excellence Cluster on Cellular Stress Responses in Aging-Associated Diseases (CECAD), University of Cologne, Faculty of Medicine and University Hospital Cologne, Cologne, Germany
[4]Research Center On Rare Kidney Diseases (RECORD), University Hospital Erlangen, Erlangen, Germany
[5]Institute of Molecular Biology and Biotechnology, Foundation for Research and Technology-Hellas, Heraklion, Crete, Greece.
[6]Division of Nephrology, Department of Internal Medicine, University of Michigan, Ann Arbor, Michigan, USA.
[7] Department of Clinical Medicine, Aarhus University, Aarhus, Denmark
[8]Department of Pediatrics-Nephrology, University of Michigan, Ann Arbor, Michigan
[9]Department of Medicine IV, Faculty of Medicine, University of Freiburg, Freiburg, Germany.
[10]Institute of Surgical Pathology, Faculty of Medicine, University of Freiburg, Freiburg, Germany.
[11]Nephrological Center, Medical Clinic and Polyclinic IV, University of Munich, Munich, Germany
[12]Department of Molecular and Cellular Sport Medicine, German Sport University Cologne, Cologne, Germany
[13]Division of Nephrology, Boston Children's Hospital, Boston, Massachusetts, USA
[14]Harvard Medical School, Boston Massachusetts, USA
[15]Broad Institute, Cambridge, Massachusetts, USA
[16]National Institute for Public Health and the Environment, Bilthoven, The Netherlands.
[17]Department of Biology, University of Crete, Heraklion, Crete, Greece.
[18]Systems Biology of Ageing Cologne, SyBaCol, University of Cologne, Germany
[19]Institute for Genome Stability in Aging and Disease, Medical Faculty, University of Cologne, Germany

Correspondence should be addressed to:

Christine E. Kurschat
Nephrology Research Lab
CECAD
University of Cologne
Joseph Stelzmann-Straße 26
50931 Cologne, Germany
Tel +49-221-478 4480
Fax +49-221-478 5959
E-mail: christine.kurschat@uk-koeln.de

Fabian Braun
E-mail: fa.braun@uke.de
Twitter: @fab_braun

Word count Abstract: 273
Word count Text: 4013

Abstract:

Background: DNA repair is essential for preserving genome integrity and ensuring cellular functionality and survival. Podocytes have a very limited regenerative capacity, and their survival is essential to maintain kidney function. While podocyte depletion is a hallmark of many glomerular diseases, the mechanisms leading to severe podocyte injury and loss remain unclear.

Methods: We investigated DNA repair mechanisms in glomerular diseases by gene expression analysis of human kidney biopsies. Using a constitutive and an inducible podocyte-specific *Ercc1* knockout mouse model, we assessed the influence of disrupted NER *in vivo,* complemented by mechanistical *in vitro* studies of induced DNA damage in cultured podocytes. Furthermore, we characterized DNA damage-related alterations in aged mice and human renal tissue of different age groups as well as in minimal change disease (MCD) and Focal segmental glomerulosclerosis (FSGS) patient biopsies.

Results: We detected perturbed NER gene expression in nuclei of podocytes in FSGS as well as aberrations of DNA repair genes in biopsies of patients with various podocyte-related glomerular diseases. Genome maintenance through NER proved to be indispensable for podocyte homeostasis. Podocyte-specific accumulation of DNA damage through the knockout of the NER endonuclease co-factor Ercc1 resulted in proteinuria, podocyte loss, glomerulosclerosis, and renal insufficiency. The response to this genomic stress was fundamentally different to the pattern reported in other cell types, as podocytes activated mTORC1 signaling upon DNA damage *in vitro* and *in vivo*. The induced mTORC1 activation was abrogated by inhibiting DNA damage response through DNA-PK and ATM *in vitro*. Moreover, pharmacological inhibition of mTORC1 ameliorated the development of glomerulosclerosis in NER-deficient mice.

Conclusion: Disruption of DNA damage response pathways seems to be a uniform response in several glomerulopathies. Accumulation of DNA damage in podocytes results in glomerulosclerosis and activates mTORC1 signaling.

Keywords:

Podocyte, DNA Damage, Ercc1, mTORC1, Glomerulosclerosis

Translational statement

Growing evidence suggests that perturbations in genome maintenance play a role in glomerulopathies. The authors have identified several DNA repair genes to be differentially expressed in glomerular diseases in human kidney biopsies and observed dramatic differences in

nucleotide excision repair (NER) gene expression in focal segmental glomerulosclerosis (FSGS) podocytes. *In vivo* and *in vitro* analyses in murine podocytes uncovered accumulation of DNA damage through disruption of NER to result in podocyte loss with glomerulosclerosis and to activate the mTORC1 pathway. Similar results were identified in FSGS patient biopsies as well as in renal specimens of human and murine aging. These findings reveal that DNA damage and its repair pathways are crucial for podocyte maintenance and for the development of glomerulosclerosis, potentially serving as therapeutic targets in the future.

Introduction:

Most cells of the body are constantly subjected to various endogenous and exogenous DNA damaging agents [1,2]. Therefore, cells depend on numerous DNA repair mechanisms to counteract genomic stress [3]. Mutations in DNA repair genes result in a variety of pathologies ranging from cancer to progeroid syndromes [4,5]. The specific importance of genome maintenance in cells with limited regenerative capacity is demonstrated by the prevalence of neurodegeneration as a hallmark of DNA repair deficiency syndromes [6].

Glomerular podocytes are terminally differentiated, post-mitotic cells with little to no replacement post-development [7]. As an integral part of the primary filtration unit of the kidney [8], podocyte depletion is a leading cause of chronic kidney disease due to diabetes, hypertension, and other glomerulopathies, with ensuing loss of protein into the urine [9]. The precise pathomechanisms leading to podocyte depletion, however, are incompletely understood. Protecting this finite number of cells is, therefore, an important therapeutic goal [10].

Lately, first studies have indicated the importance of genome maintenance for renal health [11,12]. Mutations in the kinase endopeptidase and other proteins of small size (KEOPS) complex genes caused proteinuria and induced DNA damage response (DDR) *in vitro* [13]. Likewise, glomerular DNA damage was found to be associated with declining kidney function [14] and cells isolated from the urine of patients suffering from diabetes and hypertension showed increased levels of DNA strand breaks [15]. First evidence of nucleotide excision repair (NER) being an essential pathway in kidney health was recently provided through the identification of *ERCC1* variants causing kidney dysfunction in patients [16]. However, this study mostly reported on a tubulopathy phenotype, hence, the link between DNA damage and podocyte loss remains unclear.

Several studies have proposed an interplay between DNA damage signaling and the mechanistic target of rapamycin (mTOR) pathway with factors induced by DNA damage exhibiting repressive effects on mTOR-complex1 (mTORC1) [17–19] and increased mTORC1 activity leading to genomic stress [20–22]. This is of particular interest for podocytes, as they are highly dependent on a rigorous control of mTOR activity. While mTORC1-driven hypertrophy is a protective response upon podocyte depletion [23–25], mTORC1 overactivation drives pathologic hyperproliferation and sclerosis [26,27]. In line with these findings, side effects of pharmacological mTORC1 inhibition entail proteinuria and glomerular scarring [28–34].

In this study, we identified perturbations in the expression of DNA repair genes in glomeruli from various human glomerular diseases associated with podocyte depletion and a significant loss of NER gene expression in podocytes of FSGS patients. Podocyte-specific DNA damage

accumulation through NER disruption resulted in proteinuria, podocyte loss, glomerulosclerosis, and renal insufficiency in mice. Ancillary, DNA damage accumulation was identified as a hallmark of murine and human podocyte aging. Strikingly, both *in vivo* and *in vitro* analyses revealed mTORC1 activation upon DNA damage, indicating a cell-type specific response. Inhibiting parts of the DNA damage response diminished mTORC1 activation and, in turn, inhibiting mTORC1 activation ameliorated glomerulosclerotic phenotypes in two NER-deficient mouse models. These results directly link genome maintenance to mTORC1 signaling and glomerular diseases.

Methods:

ERCB Human microarray analysis

167 genes involved in DNA repair and nucleotide excision repair were compiled from the hallmark gene set "DNA-Repair" from the Molecular Signatures Database (MSigDB) Collection[35] and upon literature research. Human kidney biopsies and Affymetrix microarray expression data were obtained within the framework of the European Renal cDNA Bank - Kröner-Fresenius Biopsy Bank [36]. Diagnostic biopsies were obtained from patients after informed consent and with approval of the local ethics committees. Following renal biopsy, the tissue was transferred to RNase inhibitor and micro-dissected into glomeruli and tubulo-interstitium. Total RNA was isolated, reverse transcribed, and amplified to a protocol previously reported [37]. Fragmentation, hybridization, staining, and imaging were performed according to the Affymetrix Expression Analysis Technical Manual (Affymetrix, Santa Clara, CA, USA). Published datasets of glomerular samples were analysed for mRNA expression levels. Analysis included datasets from patients with minimal change disease (MCD; n=14), focal segmental glomerulosclerosis (FSGS; n=23), membranous nephropathy (MGN; n=21), IgA nephropathy (Glom; n=27), and hypertensive nephropathy (HTN; n=15) as well as controls (living donors (LD); n=42) (GSE99340, LD data from: GSE32591, GSE37463). CEL file normalization was performed with the Robust Multichip Average method using RMAExpress (Version 1.0.5) and the human Entrez-Gene custom CDF annotation from Brain Array version 18 (http://brainarray.mbni.med.umich.edu/Brainarray/default.asp). To identify differentially expressed genes, the SAM (Significance Analysis of Microarrays) method [38] was applied using SAM function in Multiple Experiment Viewer (TiGR MeV, Version 4.9). A q-value below 5% was considered to be statistically significant. The resulting gene expression list was censored for genes, whose products were detected in a transcriptomic and proteomic analysis of wild-type murine podocytes [39].

Single nucleus sequencing

Nuclei were prepared from kidney biopsy cores stored in RNAlater from FSGS patients enrolled in the NEPTUNE study. The processing followed the protocol developed from the Kidney Precision Medicine Project. Nuclei preparations were processed and sequenced using 10x Genomics single cell sequencer. Analyses were performed on the output data files from CellRanger v6.0.0 using the Seurat R package (version 3.2 and 4.0; https://cran.r-project.org/web/packages/Seurat/index.html). To limit low quality nuclei and/or multiplets, we set gene counts and cutoffs to between 500 and 5000 genes and examined nuclei with a mitochondrial gene content of less than 10%. Nuclei were merged into a Seurat object using the CCA integrate function and nuclear cluster annotation was determined by finding enriched genes in each cell cluster. A comparison of these cluster selective gene profiles was compared against previously identified cell marker gene sets from human kidney samples from KPMP and other sources [40].

Mice

Mice were bred in a mixed FVB/CD1 (*Ercc1* pko) or FVB/CD1/C57BL6 (*Ercc1* ipko) background. All offspring was born in normal mendelian ratios. Mice were housed in the animal facility of the Center for Molecular Medicine Cologne or the Cluster of Excellence – Cellular Stress Responses in Aging-Associated Diseases. Following federal regulations, the Animal Care Committee of the University of Cologne reviewed and approved the experimental protocols. Animals were housed at specific pathogen-free (SPF) conditions with three-monthly monitoring according to FELASA suggestions. Housing was done in groups of less than six adult animals receiving CRM pelleted breeder and maintenance diet irradiated with 25 kGy (Special Diet Services, Witham, UK) and water *ad libitum*. Spot urine was collected once a week during cage changes or during sacrifice. Tamoxifen was administered at 400 mg/kg Tamoxifen in dry chow.

For rapamycin injection studies male and female *Ercc1*$^{fl/fl}$ (ctrl) and *Ercc1*; *pod-cre* (pko) mice at week 6 of age were injected intraperitoneally 3 times/week with 2 mg/kg bw of rapamycin diluted in 5% ethanol, 5% tween 80 and 5% PEG 400 or with 5% ethanol, 5% tween 80 and 5% PEG 400 as vehicle. Urine collection was performed 2 times/week and mice were sacrificed at week 13 of age for serum and kidney tissue isolation. All animals were maintained in grouped cages on a 12h light/dark cycle. Mice were kept on a regular diet and had access to water *ad libitum*. Body weight was measured weekly. Animals were housed in a temperature-controlled, pathogen-free animal facility at the Institute of Molecular Biology and Biotechnology (IMBB), which operates in compliance with the “Animal Welfare Act” of the Greek government, using the “Guide for the Care and Use of Laboratory Animals” as its standard.

Mice were anaesthetized by intraperitoneal injection of 10 μl per g bodyweight of 0,01% xylocaine

and 12,5 mg/ml ketamine – blood was drawn from the left ventricle into a syringe rinsed with Heparin sulfate, and animals were perfused with cold phosphate buffered saline (PBS). Kidneys were excised and embedded in OCT (Sakura, Torrance, CA) and frozen at -80°C or fixed in 4% neutral buffered formalin and subsequently embedded in paraffin.

Podocyte isolation

To isolate primary podocytes, *Ercc1*$^{fl/fl}$ mice heterozygous for the *R26mTmG* and *NPHS2.Cre* transgene were sacrificed and kidneys were used for glomerular preparation, as previously described [39]. The glomeruli were digested and the single-cell suspension was used for fluorescence-activated cell sorting.

qPCR Analysis

Total ribonucleic acid (RNA) was extracted from podocytes of *Ercc1/Pod:Cre/mTmG* mice using Direct-zol™ RNA MiniPrep Kit (cat. no. R2052, Zymo Research). Isolation of glomeruli, preparation of a glomerular single-cell suspension, and fluorescence-activated cell sorting was done as previously described [7]. Podocytes were sorted into TriReagent (cat. no. 93289, Sigma-Aldrich). The complementary deoxyribonucleic acid (cDNA) was synthesized with High Capacity cDNA Reverse Transcription Kit (cat. no. 4368814, Applied Biosystems). PCR was performed using TaqMan™ Gene Expression Master Mix (cat. no. 4369016, Applied Biosystems) and the Applied Biosystems Real-time PCR system. Real-time PCR was measured with triplicates in each gene target. The sequence of the PCR primer used for *Ercc1* was: 5′-AGCCAGACCCTGAAAACAG-3′ and 5′- CACCTCACCGAATTCCCA-3′ in PrimeTime Mini qPCR Assay for *Ercc1* (Assay-ID: Mm.PT.58.42152282, IDT). The gene expression was calculated using comparative cycle threshold method and normalized to RNA polymerase II subunit A (*Polr2a*). The relative fold change of *Ercc1* expression in knockout mice was compared with WT and heterozygous mice.

Urinary Albumin ELISA & Creatinine measurement

Urinary albumin levels were measured with a mouse albumin ELISA kit (mouse albumin ELISA kit; Bethyl Labs, Montgomery, TX, USA). Urinary creatinine kit (Cayman Chemical, Ann Arbor, MI, USA) was used to determine corresponding urinary creatinine values. For Coomassie Blue detection of albuminuria, spot urine of mice was diluted 1:20 in 1x Laemmli buffer and urinary proteins separated using poly-acrylamide gel electrophoresis with subsequent Coomassie gel stain.

Plasma Creatinine and Urea measurement

Blood samples were centrifuged at 400 g 4°C for 20 minutes and plasma samples subsequently stored at -20°C until further analysis. Creatinine and Urea were measured using standard clinical protocols by the Department of Clinical Chemistry of the University of Cologne.

Histologic analysis

To assess morphological changes in light microscopy we performed Periodic Acid Schiff staining. For specific antibody stainings sections were deparaffinized in Xylene (VWR, Darmstadt, Germany), rehydrated in decreasing concentrations of ethanol, and subjected to heat-induced antigen retrieval in 10 mM Citrate Buffer pH 6 for 15 minutes. Peroxidase blocking was performed in methanol mixed with 3% hydrogen peroxidase (Roth, Karlsruhe, Germany) followed by Avidin/Biotin Blocking (Vector, Burlingame, CA, USA) for 15 minutes each. After incubation in primary antibody (anti-phospho-S6 Ribosomal Protein (Ser235/236) # 4858 – Cell Signaling Technology) 1:200 in TBS 1% BSA at 4°C overnight, sections were washed in TBS and incubated in biotinylated secondary antibody (Jackson Immunoresearch, West Grove, USA) 1h at room temperature. For signal amplification the ABC Kit (Vector, Burlingame, CA, USA) was used before applying 3,30-diaminobenzamidine (Sigma-Aldrich, St Louis, USA) as a chromogen. Hematoxylin was used for counterstaining. After dehydration, slides were covered in Histomount (National Diagnostics, Atlanta, USA).

Immunofluorescence Staining

Paraffin embedded tissue was cut into 3 μm thick sections and processed according to published protocols [41]. Primary antibodies (anti-γH2A.X #2577s – Cell Signalling Technology, anti-nephrin #GP-N2 – Progen, anti-synaptopodin #65294 – Progen, anti-Dach1 #HPA012672 – Sigma Aldrich [42], anti-phospho-S6 Ribosomal Protein (Ser235/236) # 4858 – Cell Signaling Technology), and anti-p53 (anti-p53 #p53-protein-cm5 Leica Biosystems) were used at 1:200 dilution. Far-red fluorescent DNA dye Draq 5 was used as a nuclear marker.

Cells were processed according to published protocols [43].

For γH2A.X foci quantification, a custom-built FIJI macro was used. In brief, podocyte nuclei were identified through surrounding synaptopodin staining, segmented using the freehand tool and split into single channels. Draq 5 channel was converted into binary image using auto threshold “otsu dark” with subsequent particle measurement (range 5-Infinite) to determine nuclear area. γH2A.X channel was converted into binary image using auto threshold “MaxEntropy dark” with subsequent particle measurement (range 0.02-infinite) to determine foci number and area.

Electron Microscopy

Mice were perfused with 4% paraformaldehyde and 2% glutaraldehyde in 0.1 M sodium cacodylate, pH 7.4. Postfixation was performed in the same buffer for two additional weeks at 4°C. Tissue was osmicated with 1% OsO4 in 0.1 M cacodylate and dehydrated in increasing ethanol concentrations. Epon infiltration and flat embedding were performed following standard procedures. Toluidine blue was used to stain semithin sections of 0.5 μm. 30 nm-thick sections were cut with an Ultracut UCT ultramicrotome (Reichert) and stained with 1% aqueous uranylic acetate and lead citrate. Samples were studied with Zeiss EM 902 and Zeiss EM 109 electron microscopes (Zeiss, Oberkochen, Germany).

In vitro Experiments

Conditional immortalized murine podocytes were a gift by Stuart Shankland. Cells were cultured as previously described [44]. Briefly, immortalized podocytes were cultured in RPMI media supplemented with 10% FBS and IFNγ (Sigma-Aldrich, Taufkirchen, Germany). Cells proliferated at 33°C on Primaria plastic plates (BD Biosciences, San Jose, CA, USA) until they reached a confluence of 60-70%. Differentiation of podocytes was induced by seeding the cells at 37°C in the absence of IFNy. After 10 days of differentiation, cells were treated with 5 or10 μg/ml Mitomycin C (#M0503 - Sigma-Aldrich, Taufkirchen, Germany) for 2h in serum-free medium, followed by one washing step with Phosphate-Buffered Saline and further incubation for 6 h in serum-free medium without Mitomycin C before further processing. The absence of mycoplasm infection was tested regularly using the mycoplasm detection kit from Minerva biolabs (Minerva Biolabs, Berlin, Germany). For experiments with DNA damage response inhibitors, differentiated cells were pre-treated with 3 μM KU60019 (Selleckchem, Houston, TX, USA) or 1 μM Nedisertib (Selleckchem, Houston, TX, USA) for 1 h before inducing DNA damage by UV-C or Mitomycin C treatment. Inhibitors were added again after medium change following DNA damage induction to further incubate cells for 6 h before cell lysis.

Western Blot analysis

SDS-PAGE was used for protein size separation with subsequent blotting onto polyvinylidene difluoride membranes and visualized with enhanced chemiluminescence after incubation of the blots with corresponding antibodies (Phospho-Histone H2A.X (Ser139); Phospho-S6 Ribosomal Protein (Ser235/236) (D57.2.2E); S6 Ribosomal Protein (5G10) – Cell Signaling Technology; alpha Actin – Developmental Studies Hybridoma Bank; beta-Tubulin (E7) - Developmental Studies Hybridoma Bank).

eQTL Analysis

For the subgroup analysis of FSGS cohort, the procedure described in Gillies et al., 2018 was used with the following exceptions: only FSGS patients were analysed (N=87) and only RNAseq expression data for glomerular samples were utilized. Briefly cis-eQTLs were identified using MatrixEQTL from among variants that were located either within the annotated boundaries of a gene or its surrounding region (+/- 500 kb) [45]. We then adjusted for age, sex, principal components of genetic ancestry, and the first 5 PEER factors [46]. The genetic ancestry was calculated using LD-pruned WGS data from across all 87 patients using the EPACTS tool (https://genome.sph.umich.edu/wiki/EPACTS). The gene-level FDR for the MatrixEQTL was controlled using TORUS. Fine mapping of the eQTLs was performed using the DAP algorithm [47].

Study approval

All investigations involving human specimen have been conducted according to the Declaration of Helsinki following approval of the local ethics committees. Written informed consent was received from participants prior to inclusion in the study. All mouse experiments were conducted according to institutional and federal guidelines and approved by the LANUV NRW VSG 84-02.04.2013.A336.

Statistics

If not stated otherwise, unpaired two tailed Student's t-test was used to compare two groups and p values ≤ 0.05 were considered significant. For multiple group comparisons, we applied 1-way ANOVA followed by Tukey's post hoc correction. Statistics were performed using GraphPad Prism 8.

Results:

DNA damage repair is essential for podocyte health and is impaired in focal segmental glomerulosclerosis

To determine the involvement of the NER pathway in podocyte loss, we investigated the expression of NER genes in podocytes of FSGS biopsies, Minimal change disease (MCD) patients and controls using single nucleus sequencing. Indeed, we detected an upregulation in the *Ercc1*-8 genes, all involved in damage recognition, DNA unwinding and damage excision, in FSGS podocytes when compared to MCD and living donor kidney samples (Fig. 1A). Conversely the expression of various polymerases involved in the synthesis of new repaired strands was virtually lost in the podocytes of both MCD and FSGS samples indicative of a predominance of damage recognition and strand excision in the FSGS biopsies (Fig. S1A). Targets of the mTORC1

pathway, used as an internal control, increased in expression with little changes in the percentage of podocytes expressing these genes (Fig. S1A).

Likewise, we detected a wide array of alterations in the expression of DNA repair and NER genes in glomerular lysates of different nephropathies compared to controls (Fig. S1B; Tbl. S1) Furthermore, we assessed whether genetic variants associated with glomerular mRNA expression of DNA repair genes could be detected in patients with sclerotic glomerular diseases (Table S2) and we identified single nucleotide polymorphisms (SNPs) associated with alterations in the expression of DNA repair genes (Table S2 - S4).

As the perturbation of NER genes in FSGS podocytes could indicate defective DNA repair mechanisms, we investigated the accumulation of DNA damage in podocyte nuclei using γH2A.X immunofluorescence staining in human biopsies of FSGS compared to MCD patients. Indeed, we detected a marked increase in podocyte-specific nuclear γH2A.X foci in FSGS glomeruli (Fig. 1B & S1C, D & E), corresponding to DNA double-strand breaks and thus suggestive of an involvement of DNA damage accumulation in podocyte damage and loss.

A well-established model to induce DNA damage *in vivo* is to induce a functional impairment of the NER cascade by deletion of the endonuclease Ercc4's co-factor, the DNA excision repair protein Ercc1 [48–50]. Investigating glomeruli of the *Ercc1* -/delta mouse [51], a mouse model with whole body disruption of *Ercc1* on one allele and a truncated form of *Ercc1* on the second allele, leading to a hypomorphic variant with minimal residual activity, already revealed the development of foot process effacement at 14 weeks of age (Fig. S2A).

These findings pointed towards DNA damage repair as an essential mechanism for podocyte health. Thus, we generated a constitutive podocyte-specific knockout of *Ercc1* using the cre-loxP system in mice of mixed FVB/CD1 background [52] (Fig. S2B & 1C.). Mice carrying the podocyte-specific knockout (pko) had a decreased lifespan of 10-15 weeks, while cre negative animals (ctrl) and cre positive animals heterozygous for the floxed *Ercc1* allele (het) were investigated for up to 72 weeks without overt abnormalities (Fig. 1D & S2C & D). While weight gain after birth was normal up to week 9, *Ercc1* pko offspring displayed a pronounced decrease of weight thereafter (Fig. 1E). This weight drop was accompanied by the development of significant albuminuria as well as elevated serum creatinine and urea levels, starting at week 11 (Fig. 1F-H). At week 13, *Ercc1* pko mice had developed severe generalized renal damage, including glomerulosclerosis, interstitial fibrosis, and tubular atrophy with protein casts (Fig. 1I).

Similar results could be obtained in a tamoxifen-inducible podocyte specific knockout (ipko) of *Ercc1* (Fig. S3).

DNA damage accumulation in podocytes triggers cellular stress and podocyte loss

Ultrastructural alterations in 9-week-old constitutive *Ercc1* pko glomeruli were detectable in the form of focally effaced podocyte foot processes. These changes were not yet present in 7-week-old animals (Fig. 2A). Further evidence of podocyte stress was revealed by gradual reduction of nephrin expression, an important slit diaphragm protein, from weeks 9 to 13 (Fig. 2B & S4A). Podocyte number, glomerular hypertrophy, and podocyte density, investigated through staining of the podocyte specific proteins synaptopodin (SNP) and Dachshund Family Transcription Factor 1 (Dach1) remained within normal ranges at week 9 (Fig. 2C & S4B). In contrast, glomeruli from 11-week-old *Ercc1* pko mice clearly showed severe injury and loss of podocytes, indicated by the decrease and loss of both SNP and Dach1 (Fig. 2D). This loss of podocytes was further validated through the analysis of WT1-positive cells in 9- and 11-week-old *Ercc1* pko mice (Fig. S4C).

Foci of phosphorylated histone 2A.X (γH2A.X), a *bona fide* marker for DNA double-strand breaks, were significantly increased in both number and area in podocyte nuclei of *Ercc1* pko glomeruli at week 9 (Fig. 2E & S4D-F) compared to control animals. Strikingly, we also observed a smaller number of γH2A.X foci in almost all wildtype podocyte nuclei indicative of constant DNA damage occurrence and subsequent repair in healthy glomeruli. At later time points, single podocytes with γH2A.X signals covering larger areas of the nuclei became apparent in *Ercc1* pko glomeruli (Fig. 2F).

DNA damage accumulation in podocytes activates the mTORC1 pathway *in vivo*

Podocyte loss is tightly linked to mTORC1 activation and cellular hypertrophy of the remaining podocytes. Therefore, we investigated the timepoint of mTORC1 activation in *Ercc1* pko mice. Strikingly, we detected a significant increase in pS6RP-positive cells in *Ercc1* pko glomeruli at 9 weeks of age (Fig. 3A), a timepoint, when no evidence for podocyte loss was present yet (Fig. 2C & S4C). In-detail analysis revealed that more than 40% of podocytes showed mTORC1 activation at week 9 (Fig. 3A).

To investigate whether increased mTORC1 signaling contributes to the development of podocyte loss, we analysed the kidneys of *Ercc1* -/delta mice treated with 14 mg/kg food of the mTORC1 inhibitor rapamycin from 8 weeks of age until termination of the experiment due to high moribund scoring [53]. Despite the fact that the treated cohort did not present with an extended lifespan, moribund animals of the end-of-life cohort (aged 15-26 weeks) presented with a significant reduction of sclerotic glomeruli, when treated with rapamycin (Fig. 3B). Additionally, we treated

our podocyte-specific *Ercc1* ko mouse model with 2 mg/kg bodyweight rapamycin via i.p. injections three times a week, beginning at 6 weeks of age. Again, we detected a significant reduction in globally sclerotic glomeruli and more healthy glomeruli upon rapamycin treatment at the end of our observation period at week 13 (Fig. 3C).

The observed detection of increased mTORC1 signaling and DNA damage accumulation suggests a potential interplay. It has been suggested that increased mTORC1 signaling decreases the cellular ability to repair DNA damage [20,21]. Thus, we investigated the occurrence of γH2A.X foci accumulation in a podocyte-specific *Tsc1* knockout mouse model characterized by podocyte-specific mTORC1 hyperactivation [25,54]. Indeed, *Tsc1* pko mice also depicted an increased number of DNA damage foci as early as 4 weeks of age, when the phenotype is predominantly driven by mTORC1 hyperactivation (Fig. 3D).

This data indicates increased mTORC1 signaling through DNA damage accumulation and decreased DNA damage repair upon mTORC1 activation potentially constituting a downward spiral aggravating podocyte damage (Fig. 3E).

DNA damage activates the mTORC1 cascade through DNA damage signaling kinase DNA-PK in podocytes

To further investigate the mechanism behind mTORC1 activation occurring in podocytes upon genomic stress, we induced DNA damage through mitomycin C (MMC) treatment and UV-C irradiation *in vitro* in immortalized mouse podocytes (Fig. 4A). These treatments led to significant increases of γH2A.X (Fig. 4B) and accumulation of the DNA damage response protein p53 in the nucleus (Fig. 4C). Again, DNA damage induced an increased phosphorylation of S6 ribosomal protein (pS6RP), which is a downstream target of mTORC1, in podocytes (Fig. 4D). This phosphorylation was completely abrogated by mTORC1 inhibitor rapamycin and reduced by serum starvation, a well-known mTORC1 modulator[55]. In order to identify the link between DNA damage accumulation and mTORC1 activation, we treated MMC- or UV-C-stimulated murine podocytes with inhibitors of the DNA damage signaling cascade (Fig. 4E). In both conditions, inhibition of DNA-dependent protein kinase (DNA-PK) by Nedisertib resulted in abrogation of S6RP phosphorylation. Similar results could be achieved with the Ataxia Telangiectasia Mutated serine/threonine kinase (ATM) inhibitor KU60019. No effects were detected upon treatment with the ATR inhibitor VE822 or with the CHK1 inhibitor prexasertib (data not shown). These data indicate a direct mechanistic link between genomic stress and mTORC1 signaling in podocytes.

Since genomic stress represents a hallmark of cellular aging, we investigated both murine and human glomeruli of young and aged subjects. Indeed, the well-documented increase in mTORC1 signaling in aged murine podocytes coincided with increased detection of DNA damage foci (Fig. 4F & S5A). Similar results were detected in a series of human tumor nephrectomy samples when comparing a young group (21-49 years; n=4) with an old group (69-81 years; n=5) (Fig.4G & S5B). These results validate the occurrence of DNA damage in both healthy murine and human podocytes and indicate an association between DNA damage and aging in podocytes, possibly contributing to age-related podocyte loss [25].

Discussion:

Our study allows two principal conclusions: (1) DNA repair mechanisms are involved in the pathophysiology of glomerular disease, which are indispensable for podocyte homeostasis, and (2) podocytes respond to DNA damage by upregulation of the mTORC1 pathway in a DNA-PK-mediated manner before the onset of podocyte loss, not via a repression of the mTORC1 pathway. Together, this is the first report drawing a connection between DNA repair mechanisms and glomerular diseases via mTORC1 signaling.

Only recently the importance of DNA repair has sparked larger interest in the field of podocyte biology. Due to their often deleterious clinical phenotypes in humans, the description of glomerular abnormalities in syndromes caused by mutations in DNA repair genes is scarce [56,57]. However, there is evidence for podocyte involvement in syndromes caused by mutations of DNA repair genes underlined by reports of patients exhibiting proteinuria and nephrotic syndrome [49,58,59]. The same holds true for factors involved in other forms of DNA maintenance such as the KEOPS complex [13,60] or KAT5, a contributor to DNA methylation and non-homologous endjoining repair [61]. Itoh and co-workers linked proteinuric kidney diseases due to hypertension and diabetes to DNA double-strand breaks and methylation in the promotor region of the slit diaphragm protein nephrin and established an association to DNA double-strand breaks in glomeruli of patients suffering from IgA nephropathy [14,15]. Our analysis adds considerably to this body of evidence, as we identify multiple factors of DNA maintenance, in particular of NER, to be transcriptionally altered in glomeruli of different renal diseases involving pronounced podocyte damage and loss. This is in line with decreased expression of NER endonuclease ERCC4 in IgA nephropathy[14]. The precise evaluation of perturbations in every single one of the identified genes goes beyond the scope of this manuscript, but we delineated the striking decrease of NER gene expression in FSGS

podocytes and investigated the podocyte-specific reaction to accumulating DNA damage in depth *in vivo* and *in vitro*.

To what extent glomerular epithelial cells are subjected to genomic stress is currently unclear. For the first time, this study reveals the occurrence of individual DNA damage foci in podocytes under healthy conditions indicating a need for constant DNA maintenance and repair in this specialized cell type. This finding is in line with studies investigating glomerular expression profiles of a partial *Ercc1* knockout [62] and an adipose tissue-specific *Ercc1* knockout that described a low amount of DNA damage foci also occurring in adipocytes of control animals [50]. A major factor contributing to this stress may result from damaging agents in the serum, as serum components are constantly filtered into the primary urine in which the podocytes are emerged in. Since podocytes entail very little capacity for regeneration [7], they are in specific need for efficient repair of occurring DNA damage and particularly vulnerable to abrogation of these repair pathways. Deficiency in the repair of DNA damage seems to be compensable up to a certain threshold as podocyte loss, proteinuria, and glomerular sclerosis only became apparent after week 9 in our mouse model. In line with these findings, decreased *Ercc1* gene expression in heterozygous mice appears to be sufficient to maintain healthy glomeruli, as these animals depict no phenotype at one year of age. Yet, the presence of foot process effacement and glomerulosclerosis in *Ercc1* -/delta mice indicates that minimal residual activity is not sufficient for podocyte health.

The interplay of DNA damage, its repair, and the mTOR pathway has been a subject of numerous studies, specifically in the field of cancer biology. These studies indicated that mTORC1 signaling is inhibited upon DNA damage in a TSC, Sestrin or AKT dependent manner [17,18,19]. Strikingly, we observed that podocytes both *in vitro* and *in vivo* reacted to endogenous accumulation or exogenous infliction of DNA damage with activation of the mTORC1 pathway. Herein lies a fundamental difference to past reports and a potential disease mechanism as numerous studies have depicted the importance of a tight regulation of mTORC1 for podocyte health and the deleterious effects of both overactivation and repression in disease [23,25,26,43,63,64]. Since mTORC1 activation occurs in *Ercc1* pko podocytes at 9 weeks, a time point of no overt podocyte loss, mild ultrastructural differences, and significant accumulation of DNA damage foci, our data indicate a direct link between genomic stress and mTORC1 activation in podocytes via activation of DNA-PK.

A growing body of evidence suggests that mTORC1 activity reduces the capacity of successful DNA repair [20,21], e.g. through ribosomal S6 kinase (S6K)-dependent phosphorylation of E3 ubiquitin-protein ligase RNF168 [22]. However, upon podocyte depletion, remaining podocytes on

the glomerular tuft counteract the loss of neighbouring cells through mTORC1-mediated hypertrophy [25] which impairs proper DNA repair. This fact is underlined by podocyte-specific *Tsc1* knockout animals displaying mTORC1 hyperactivation, which accumulate a significantly increased amount of DNA damage foci already at 4 weeks of age. We, therefore, hypothesize that this reaction can lead to a downward spiral of insufficient DNA maintenance further aggravated through mTORC1 activation and, despite of mTORC1 mediated hypertrophy, trigger excessive podocyte loss. This cascade could potentially be ameliorated through well-timed mTORC1 inhibition as indicated by the reduction of glomerulosclerosis in rapamycin-treated *Ercc1* -/delta and *Ercc1* pko animals or upregulation of DNA repair mechanisms to alleviate accumulated genomic stress. Potential sites in the genome that could be used to alter glomerular damage repair were already identified in our eQTL analysis in FSGS patients. This is of particular interest since there seems to be a broad interplay between gene products exerting functions beyond their canonical pathways in genome maintenance [65]. Likewise, decreased expression of DNA repair genes in a subset of patients or the accumulation of DNA damage through the aging process may lead to increased mTORC1 activation in podocytes, thereby rendering a subgroup of patients vulnerable to the development of glomerular disease and scarring.

The importance of DNA damage repair in podocyte homeostasis is consistent with the role in other postmitotic cell types and particularly apparent in neurodegenerative pathologies typical for NER deficiency syndromes [5]. The role of NER in repairing transcription-blocking lesions might thus play a pivotal role in podocytes that need to maintain the integrity of transcribed genes during the entire lifespan of the organism. Even hepatocytes of *Ercc1* -/delta mice, usually characterized by high self-renewing potential, showed a considerable block of transcription, indicative of transcription-coupled mechanisms being stalled [66,47].

In conclusion, we identified nucleotide excision repair as an essential mechanism of DNA maintenance in podocyte homeostasis. The presented study characterizes the activation of mTORC1 signaling as a podocyte-specific response to DNA damage and identifies the accumulation of DNA damage as one novel hallmark of podocyte loss and glomerular disease, suitable for precision medicine approaches.

Disclosures:

The authors declare no conflict of interest.

Author contributions:

FB, AMM, LB, RAH, VGP, MNW, GC, MR, DF, GGS, SK, MTL, WB, VN, PM performed experiments; FB, LB, AMM, GC, RAH, VGP, MNW, DF, MTL, WB, MGS, VN analysed data; FB, AMM, VGP, GG, MD, PTB, CDC, MK, MGS, MK, TBH, BSche, TB, BSchu, CEK conceived experiments, FB, VGP, BSchu, CEK wrote the manuscript, all authors revised the manuscript, all authors agreed on the publication in the presented state.

Funding:

Fabian Braun received funding from the Else-Kröner-Fresenius-Stiftung: Else-Kröner-Memorial Stipendium / 2021_EKMS.26

Amrei M. Mandel was partially funded by the Else Kröner-Fresenius-Stiftung and the Eva Luise und Horst Köhler Stiftung – Project No: 2019_KollegSE.04.

Linda Blomberg was supported by the Faculty of Medicine, of University of Cologne: Koeln Fortune Program KF 12/2020.

Victor Puelles received support from the Deutsche Forschungsgemeinschaft: Clinical Research Unit / CRC1192, and the Bundesministerium für Bildung und Forschung eMed Consortia / Fibromap) and the Novo Nordisk Foundation (NNF21OC0066381).

Georgia Chatzinikolaou is supported by ELIDEK grant agreement No 1059, funded from the Hellenic Foundation for Research and Innovation (HFRI) and the General Secretariat for Research and Technology (GSRT).

Gisela G. Slaats was supported by an EMBO long-term fellowship ALTF 475-2016 and the Fritz Thyssen Foundation project 10.20.1.012MN.

Martijn Dollé received support the National Institute of Health (NIH)/National Institute of Aging (NIA) (AG17242)

Paul T. Brinkoetter received support from the Deutsche Forschungsgemeinschaft: Clinical research unit: KFO 329, BR 2955/8-1, and the Bundesministerium für Bildung und Forschung STOP-FSGS 01GM1901E

Matthew G. Samspon is supported by NIH grants RO1 DK108805, DK119380, and RC2 DK122397

George A. Garinis was supported by ELIDEK grant 631, funded from the Hellenic Foundation for Research and Innovation (HFRI).

The George M. O'Brien Michigan Kidney Translational Core Center was funded by NIH/NIDDK grant 2P30-DK-081943.

Bernhard Schermer received support by the Deutsche Forschungsgemeinschaft: Clinical research unit KFO 329 SCHE 1562/7-1.

Thomas Benzing received support from the Deutsche Forschungsgemeinschaft: Clinical research unit: KFO 329, BE 2212/23-1 & 2212/24-1, and the Bundesministerium für Bildung und Forschung STOP-FSGS 01GM1901E

Christine Kurschat received support by the Deutsche Forschungsgemeinschaft: Clinical research unit KFO 329 KU 1539/5-1.

References:

1. Lindahl T, Nyberg B: Rate of depurination of native deoxyribonucleic acid. *Biochemistry-us* 11: 3610–3618, 1972
2. Loeb LA, Harris CC: Advances in chemical carcinogenesis: a historical review and prospective. *Cancer Res* 68: 6863–72, 2008
3. Chatterjee N, Walker GC: Mechanisms of DNA damage, repair, and mutagenesis: DNA Damage and Repair. *Environ Mol Mutagen* 58: 235–263, 2017
4. Ghosal G, Chen J: DNA damage tolerance: a double-edged sword guarding the genome. *Transl Cancer Res* 2: 107–129, 2013
5. Wolters S, Schumacher B: Genome maintenance and transcription integrity in aging and disease. *Frontiers Genetics* 4: 19, 2013
6. Madabhushi R, Pan L, Tsai L-H: DNA damage and its links to neurodegeneration. *Neuron* 83: 266–82, 2014
7. Wanner N, Hartleben B, Herbach N, Goedel M, Stickel N, Zeiser R, et al.: Unraveling the role of podocyte turnover in glomerular aging and injury. *Journal of the American Society of Nephrology : JASN* 25: 707–716, 2014
8. Butt L, Unnersjö-Jess D, Höhne M, Edwards A, Binz-Lotter J, Reilly D, et al.: A molecular mechanism explaining albuminuria in kidney disease. *Nat Metabolism* 2: 461–474, 2020
9. Chen TK, Knicely DH, Grams ME: Chronic Kidney Disease Diagnosis and Management. *Jama* 322: 1294–1304, 2019
10. Rosenberg AZ, Kopp JB: Focal Segmental Glomerulosclerosis. *Clinical journal of the American Society of Nephrology : CJASN* 12: 502–517, 2017
11. Marshall CB, Pippin JW, Krofft RD, Shankland SJ: Puromycin aminonucleoside induces oxidant-dependent DNA damage in podocytes in vitro and in vivo. *Kidney Int* 70: 1962–1973, 2006
12. Hakroush S, Cebulla A, Schaldecker T, Behr D, Mundel P, Weins A: Extensive Podocyte Loss Triggers a Rapid Parietal Epithelial Cell Response. *Journal of the American Society of Nephrology : JASN* 25: 927–938, 2014
13. Braun DA, Rao J, Mollet G, Schapiro D, Daugeron M-C, Tan W, et al.: Mutations in KEOPS-complex genes cause nephrotic syndrome with primary microcephaly. *Nature genetics* 49: 1529–1538, 2017
14. Hayashi K, Hishikawa A, Hashiguchi A, Azegami T, Yoshimoto N, Nakamichi R, et al.: Association of glomerular DNA damage and DNA methylation with one-year eGFR decline in IgA nephropathy. *Sci Rep-uk* 10: 237, 2020

15. Hishikawa A, Hayashi K, Yoshimoto N, Nakamichi R, Homma K, Itoh H: DNA damage and expression of DNA methylation modulators in urine-derived cells of patients with hypertension and diabetes. *Sci Rep-uk* 10: 3377, 2020
16. Apelt K, White SM, Kim HS, Yeo J-E, Kragten A, Wondergem AP, et al.: ERCC1 mutations impede DNA damage repair and cause liver and kidney dysfunction in patients. *J Exp Med* 218: 2020
17. Reiling JH, Hafen E: The hypoxia-induced paralogs Scylla and Charybdis inhibit growth by down-regulating S6K activity upstream of TSC in Drosophila. *Gene Dev* 18: 2879–2892, 2004
18. Budanov AV, Karin M: p53 Target Genes Sestrin1 and Sestrin2 Connect Genotoxic Stress and mTOR Signaling. *Cell* 134: 451–460, 2008
19. Wu D-D, Gao Y-R, Li T, Wang D-Y, Lu D, Liu S-Y, et al.: PEST-containing nuclear protein mediates the proliferation, migration, and invasion of human neuroblastoma cells through MAPK and PI3K/AKT/mTOR signaling pathways. *Bmc Cancer* 18: 499, 2018
20. Chebel A, Catallo R, Mabon C, Bachy E, Wenner T, Salles G, et al.: Rapamycin safeguards lymphocytes from DNA damage accumulation in vivo. *European journal of cell biology* 95: 331–341, 2016
21. Dominick G, Bowman J, Li X, Miller RA, Garcia GG: mTOR regulates the expression of DNA damage response enzymes in long-lived Snell dwarf, GHRKO, and PAPPA-KO mice. *Aging Cell* 16: 52–60, 2016
22. Xie X, Hu H, Tong X, Li L, Liu X, Chen M, et al.: The mTOR–S6K pathway links growth signalling to DNA damage response by targeting RNF168. *Nat Cell Biol* 20: 320–331, 2018
23. Zschiedrich S, Bork T, Liang W, Wanner N, Eulenbruch K, Munder S, et al.: Targeting mTOR Signaling Can Prevent the Progression of FSGS. *Journal of the American Society of Nephrology : JASN* 28: 2144–2157, 2017
24. Nishizono R, Kikuchi M, Wang SQ, Chowdhury M, Nair V, Hartman J, et al.: FSGS as an Adaptive Response to Growth-Induced Podocyte Stress. *Journal of the American Society of Nephrology : JASN* 28: 2931–2945, 2017
25. Puelles VG, Wolde JW van der, Wanner N, Scheppach MW, Cullen-McEwen LA, Bork T, et al.: mTOR-mediated podocyte hypertrophy regulates glomerular integrity in mice and humans. *Jci Insight* 4: e99271, 2019
26. Inoki K, Mori H, Wang J, Suzuki T, Hong S, Yoshida S, et al.: mTORC1 activation in podocytes is a critical step in the development of diabetic nephropathy in mice. *The Journal of clinical investigation* 121: 2181–2196, 2011
27. Kurayama R, Ito N, Nishibori Y, Fukuhara D, Akimoto Y, Higashihara E, et al.: Role of amino acid transporter LAT2 in the activation of mTORC1 pathway and the pathogenesis of crescentic glomerulonephritis. *Lab Invest* 91: 992–1006, 2011
28. Dittrich E, Schmaldienst S, Soleiman A, Horl WH, Pohanka E: Rapamycin-associated post-transplantation glomerulonephritis and its remission after reintroduction of calcineurin-inhibitor therapy. *Transplant Int* 17: 215–220, 2004
29. Butani L: Investigation of Pediatric Renal Transplant Recipients with Heavy Proteinuria after Sirolimus Rescue. *Transplantation* 78: 1362–1366, 2004
30. Izzedine H, Brocheriou I, Frances C: Post-Transplantation Proteinuria and Sirolimus. *New Engl J Med* 353: 2088–2089, 2005
31. Sennesael JJ, Bosmans JL, Bogers JP, Verbeelen D, Verpooten GA: Conversion from Cyclosporine to Sirolimus in Stable Renal Transplant Recipients. *Transplantation* 80: 1578–1585, 2005
32. Letavernier E, Bruneval P, Mandet C, Huyen J-PDV, Péraldi M-N, Helal I, et al.: High Sirolimus Levels May Induce Focal Segmental Glomerulosclerosis De Novo. *Clin J Am Soc Nephro* 2: 326–333, 2007

33. Cho ME, Hurley JK, Kopp JB: Sirolimus Therapy of Focal Segmental Glomerulosclerosis Is Associated With Nephrotoxicity. *Am J Kidney Dis* 49: 310–317, 2007
34. Hochegger K, Jansky GL, Soleiman A, Wolf AM, Tagwerker A, Seger C, et al.: Differential Effects of Rapamycin in Anti-GBM Glomerulonephritis. *J Am Soc Nephrol* 19: 1520–1529, 2008
35. Liberzon A, Birger C, Thorvaldsdóttir H, Ghandi M, Mesirov JP, Tamayo P: The Molecular Signatures Database Hallmark Gene Set Collection. *Cell Syst* 1: 417–425, 2015
36. Cohen CD, Frach K, Schlöndorff D, Kretzler M: Quantitative gene expression analysis in renal biopsies: A novel protocol for a high-throughput multicenter application. *Kidney Int* 61: 133–140, 2002
37. Cohen CD, Klingenhoff A, Boucherot A, Nitsche A, Henger A, Brunner B, et al.: Comparative promoter analysis allows de novo identification of specialized cell junction-associated proteins. *Proc National Acad Sci* 103: 5682–5687, 2006
38. Tusher VG, Tibshirani R, Chu G: Significance analysis of microarrays applied to the ionizing radiation response. *Proceedings of the National Academy of Sciences of the United States of America* 98: 5116–5121, 2001
39. Rinschen MM, Gödel M, Grahammer F, Zschiedrich S, Helmstädter M, Kretz O, et al.: A Multi-layered Quantitative In Vivo Expression Atlas of the Podocyte Unravels Kidney Disease Candidate Genes. *Cell reports* 23: 2495–2508, 2018
40. Mariani LH, Eddy S, AlAkwaa FM, McCown PJ, Harder JL, Martini S, et al.: Multidimensional Data Integration Identifies Tumor Necrosis Factor Activation in Nephrotic Syndrome: A Model for Precision Nephrology. *Medrxiv* 2021.09.09.21262925, 2021
41. Puelles VG, Douglas-Denton RN, Cullen-McEwen LA, Li J, Hughson MD, Hoy WE, et al.: Podocyte Number in Children and Adults: Associations with Glomerular Size and Numbers of Other Glomerular Resident Cells. *J Am Soc Nephrol* 26: 2277–2288, 2015
42. Endlich N, Kliewe F, Kindt F, Schmidt K, Kotb AM, Artelt N, et al.: The transcription factor Dach1 is essential for podocyte function. *J Cell Mol Med* 22: 2656–2669, 2018
43. Liebau MC, Braun F, Höpker K, Weitbrecht C, Bartels V, Müller R-U, et al.: Dysregulated Autophagy Contributes to Podocyte Damage in Fabry's Disease. *Plos One* 8: e63506, 2013
44. Shankland SJ, Pippin JW, Reiser J, Mundel P: Podocytes in culture: past, present, and future. *Kidney international* 72: 26–36, 2007
45. Shabalin AA: Matrix eQTL: ultra fast eQTL analysis via large matrix operations. *Bioinformatics* 28: 1353–1358, 2012
46. Stegle O, Parts L, Durbin R, Winn J: A Bayesian Framework to Account for Complex Non-Genetic Factors in Gene Expression Levels Greatly Increases Power in eQTL Studies. *Plos Comput Biol* 6: e1000770, 2010
47. Wen X, Lee Y, Luca F, Pique-Regi R: Efficient Integrative Multi-SNP Association Analysis via Deterministic Approximation of Posteriors. *Am J Hum Genetics* 98: 1114–1129, 2016
48. Niedernhofer LJ, Garinis GA, Raams A, Lalai AS, Robinson AR, Appeldoorn E, et al.: A new progeroid syndrome reveals that genotoxic stress suppresses the somatotroph axis. *Nature* 444: 1038–1043, 2006
49. Doig J, Anderson C, Lawrence NJ, Selfridge J, Brownstein DG, Melton DW: Mice with skin-specific DNA repair gene (Ercc1) inactivation are hypersensitive to ultraviolet irradiation-induced skin cancer and show more rapid actinic progression. *Oncogene* 25: 6229–6238, 2006
50. Karakasilioti I, Kamileri I, Chatzinikolaou G, Kosteas T, Vergadi E, Robinson AR, et al.: DNA Damage Triggers a Chronic Autoinflammatory Response, Leading to Fat Depletion in NER Progeria. *Cell Metabolism* 18: 403–415, 2013
51. Weeda G, Donker I, Wit J de, Morreau H, Janssens R, Vissers CJ, et al.: Disruption of mouse ERCC1 results in a novel repair syndrome with growth failure, nuclear abnormalities and senescence. *Current biology : CB* 7: 427–439, 1997

52. Moeller MJ, Sanden SK, Soofi A, Wiggins RC, Holzman LB: Podocyte-specific expression of cre recombinase in transgenic mice. *Genesis (New York, N.Y. : 2000)* 35: 39–42, 2003
53. Birkisdóttir MB, Jaarsma D, Brandt RMC, Barnhoorn S, Vliet N, Imholz S, et al.: Unlike dietary restriction, rapamycin fails to extend lifespan and reduce transcription stress in progeroid DNA repair-deficient mice. *Aging Cell* 20: e13302, 2021
54. Bork T, Liang W, Yamahara K, Lee P, Tian Z, Liu S, et al.: Podocytes maintain high basal levels of autophagy independent of mtor signaling. *Autophagy* 16: 1–17, 2019
55. Settembre C, Fraldi A, Medina DL, Ballabio A: Signals from the lysosome: a control centre for cellular clearance and energy metabolism. *Nature Reviews Molecular Cell Biology* 14: 283–296, 2013
56. Hirooka M, Hirota M, Kamada M: Renal lesions in Cockayne syndrome. *Pediatr Nephrol* 2: 239–243, 1988
57. Chehida AB, Ghali N, Abdelaziz RB, Moussa FB, Tebib N: Renal Involvement in 2 Siblings With Cockayne Syndrome. *Iran J Kidney Dis* 11: 253–255, 2017
58. Faridounnia M, Wienk H, Kovačič L, Folkers GE, Jaspers NGJ, Kaptein R, et al.: The Cerebro-Oculo-Facio-Skeletal (COFS) Syndrome point mutation F231L in the ERCC1 DNA repair protein causes dissociation of the ERCC1-XPF complex. *Journal of Biological Chemistry* 2015
59. Kondo D, Noguchi A, Tamura H, Tsuchida S, Takahashi I, Kubota H, et al.: Elevated Urinary Levels of 8-Hydroxy-2'-deoxyguanosine in a Japanese Child of Xeroderma Pigmentosum/Cockayne Syndrome Complex with Infantile Onset of Nephrotic Syndrome. *Tohoku J Exp Medicine* 239: 231–5, 2016
60. Hecker A, Graille M, Madec E, Gadelle D, Le Cam E, van Tilbergh H, et al.: The universal Kae1 protein and the associated Bud32 kinase (PRPK), a mysterious protein couple probably essential for genome maintenance in Archaea and Eukarya. *Biochem Soc T* 37: 29–35, 2009
61. Hishikawa A, Hayashi K, Abe T, Kaneko M, Yokoi H, Azegami T, et al.: Decreased KAT5 Expression Impairs DNA Repair and Induces Altered DNA Methylation in Kidney Podocytes. *Cell reports* 26: 1318-1332.e4, 2019
62. Schermer B, Bartels V, Frommolt P, Habermann B, Braun F, Schultze JL, et al.: Transcriptional profiling reveals progeroid Ercc1-/Δ mice as a model system for glomerular aging. *Bmc Genomics* 14: 559, 2013
63. Gödel M, Hartleben B, Herbach N, Liu S, Zschiedrich S, Lu S, et al.: Role of mTOR in podocyte function and diabetic nephropathy in humans and mice. *The Journal of clinical investigation* 121: 2197–2209, 2011
64. Ising C, Koehler S, Brähler S, Merkwirth C, Höhne M, Baris OR, et al.: Inhibition of insulin/IGF-1 receptor signaling protects from mitochondria-mediated kidney failure. *EMBO Molecular Medicine* 7: 275–287, 2015
65. Mulderrig L, Garaycoechea JI: XPF-ERCC1 protects liver, kidney and blood homeostasis outside the canonical excision repair pathways. *Plos Genet* 16: e1008555, 2020
66. Milanese C, Bombardieri CR, Sepe S, Barnhoorn S, Payán-Goméz C, Caruso D, et al.: DNA damage and transcription stress cause ATP-mediated redesign of metabolism and potentiation of anti-oxidant buffering. *Nat Commun* 10: 4887, 2019

Acknowledgments:

The excellent technical expertise of Martyna Brütting, Melanie Schaper, Anja Obser, Ilka Edenhofer and Bhawani Nagarajah is gratefully acknowledged. The DNA damage response inhibitors used in this study were a kind gift of Ron Jachimowicz. All schematics in figures were

created with BioRender.com. The ERCB-KFB was supported by the Else Kröner-Fresenius Foundation. We also thank all participating centres of the European Renal cDNA Bank - Kröner-Fresenius biopsy bank (ERCB-KFB) and their patients for their cooperation. Active members at the time of the study see (N. Shved et al., Scientific reports 7, 8576 (2017)). The Nephrotic Syndrome Rare Disease Clinical Research Network III (NEPTUNE) is part of the Rare Diseases Clinical Research Network (RDCRN), which is funded by the National Institutes of Health (NIH) and led by the National Center for Advancing Translational Sciences (NCATS) through its Office of Rare Diseases Research (ORDR). NEPTUNE is funded under grant number U54DK083912 as a collaboration between NCATS and the National Institute of Diabetes and Digestive and Kidney Diseases (NIDDK). Additional funding and/or programmatic support for this project has also been provided by the University of Michigan, NephCure Kidney International and the Halpin Foundation. All RDCRN consortia are supported by the network's Data Management and Coordinating Center (DMCC) (U2CTR002818). Funding support for the DMCC is provided by NCATS and the National Institute of Neurological Disorders and Stroke (NINDS).

Members of the Nephrotic Syndrome Study Network (NEPTUNE)

Members of the Nephrotic Syndrome Study Network (NEPTUNE)

NEPTUNE Enrolling Centers

Cleveland Clinic, Cleveland, OH: K Dell*, J Sedor**, M Schachere#, J Negrey#

Children's Hospital, Los Angeles, CA: K Lemley*, S Tang#

Children's Mercy Hospital, Kansas City, MO: T Srivastava*, S Morrison#

Cohen Children's Hospital, New Hyde Park, NY: C Sethna*, M Pfaiff #

Columbia University, New York, NY: P Canetta*, A Pradhan#

Emory University, Atlanta, GA: L Greenbaum*, C Wang**, E Yun#

Harbor-University of California Los Angeles Medical Center: S Adler*, J LaPage#

John H. Stroger Jr. Hospital of Cook County, Chicago, IL: A Athavale*, M Itteera

Johns Hopkins Medicine, Baltimore, MD: M Atkinson*, T Dell#

Mayo Clinic, Rochester, MN: F Fervenza*, M Hogan**, J Lieske*, V Chernitskiy#

Montefiore Medical Center, Bronx, NY: F Kaskel*, M Ross*, P Flynn#

NIDDK Intramural, Bethesda MD: J Kopp*, J Blake#

New York University Medical Center, New York, NY: L Malaga-Dieguez*, O Zhdanova**, F Modersitzki#, L Pehrson#

Stanford University, Stanford, CA: R Lafayette*, B Yeung#

Temple University, Philadelphia, PA: I Lee*, S Quinn-Boyle#

University Health Network Toronto: H Reich *, M Hladunewich**, P Ling[#], M Romano[#]

University of Miami, Miami, FL: A Fornoni[*], C Bidot[#]

University of Michigan, Ann Arbor, MI: M Kretzler[*], D Gipson*, A Williams[#], C Klida[#]

University of North Carolina, Chapel Hill, NC: V Derebail[*], K Gibson[*], A Froment[#], S Kelley[#]

University of Pennsylvania, Philadelphia, PA: L Holzman[*], K Meyers**, K Kallem[#], A Swenson[#]

University of Texas Southwestern, Dallas, TX: K Sambandam[*], K Aleman[#], M Rogers[#]

University of Washington, Seattle, WA: A Jefferson[*], S Hingorani**, K Tuttle**[§], M Bray[#], E Pao[#], A Cooper[#§]

Wake Forest University Baptist Health, Winston-Salem, NC: JJ Lin*, Stefanie Baker[#]

Data Analysis and Coordinating Center: M Kretzler*, L Barisoni**, C Gadegbeku**, B Gillespie**, D Gipson**, L Holzman**, L Mariani**, M Sampson**, J Sedor**, J Zee**, G Alter, H Desmond, S Eddy, D Fermin, M Larkina, S Li, S Li, CC Lienczewski, T Mainieri, R Scherr, A Smith, A Szymanski, A Williams.

Digital Pathology Committee: Carmen Avila-Casado (University Health Network, Toronto), Serena Bagnasco (Johns Hopkins University), Joseph Gaut (Washington University in St Louis), Stephen Hewitt (National Cancer Institute), Jeff Hodgin (University of Michigan), Kevin Lemley (Children's Hospital of Los Angeles), Laura Mariani (University of Michigan), Matthew Palmer (University of Pennsylvania), Avi Rosenberg (Johns Hopkins University), Virginie Royal (University of Montreal), David Thomas (University of Miami), Jarcy Zee (University of Pennsylvania) Co-Chairs: Laura Barisoni (Duke University) and Cynthia Nast (Cedar Sinai).

*Principal Investigator; **Co-investigator; [#]Study Coordinator

[§]Providence Medical Research Center, Spokane, WA

Figures and Figure Legends:

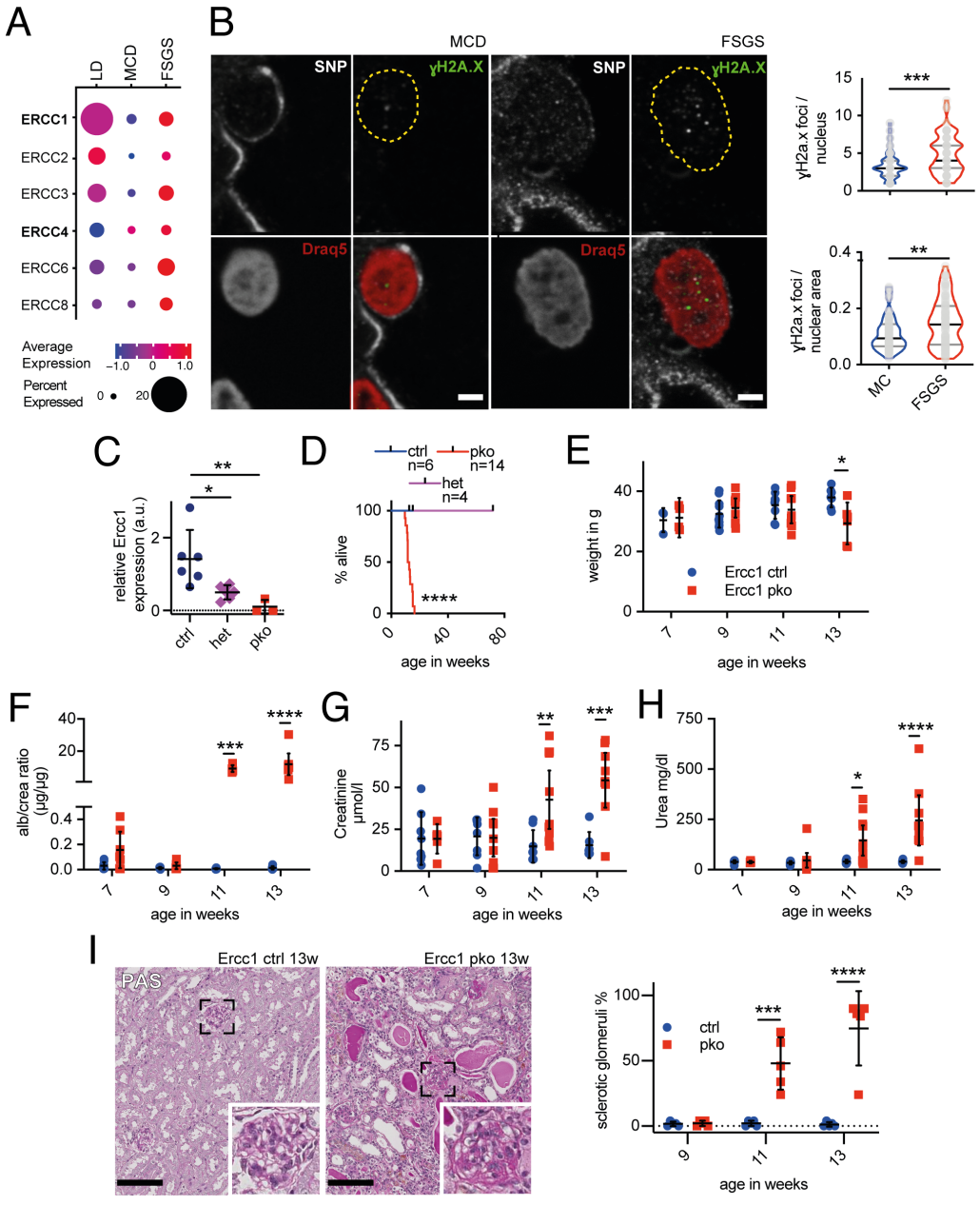

Figure 1: Nucleotide excision repair (NER) gene expression is perturbed in human FSGS and this perturbation causes glomerulosclerosis

A: Bubble plot indicating the differences in Ercc gene expression in podocytes between living donor (LD) kidney samples, Minimal change disease (MCD) and FSGS biopsies obtained through single nucleus sequencing.

B: Representative immunofluorescence staining of synaptopodin (SNP), γH2A.X and Draq5 in sections of human MCD and FSGS biopsies with quantification of γH2A.X foci per podocyte nucleus, scalebar indicating 2 μm, yellow dotted line indicating nuclear border, n=4, 4 glomeruli per sample, 5 podocytes per glomerulus.

C: qPCR analysis for *Ercc1* in FACS-sorted podocytes of *Ercc1* ctrl, wt/pko (het) or pko mice. Delta-Delta-CT values expressed as scatterplots depicting mean plus 95% confidence interval.

D: Kaplan-Meyer curve depicting survival of *Ercc1* ctrl, wt/pko (het) and pko mice (Mantel-Cox test).

E: Weight analysis; F: urinary albumin/creatinine analysis; G: serum creatinine analysis; H: serum urea analysis of *Ercc1* ctrl and pko mice.

I: Representative Periodic Acid Schiff (PAS) staining of 13-week-old *Ercc1* ctrl and pko mice and quantification of sclerotic glomeruli, scalebars: 100 μm, n = 5, 50 glomeruli per sample.

All violin plots indicate median (black) and upper and lower quartile (gray), scatterplots indicate mean plus 95% confidence interval, *p ≤ 0,05, **p ≤ 0,01, ***p ≤ 0,001, ****p ≤ 0,0001.

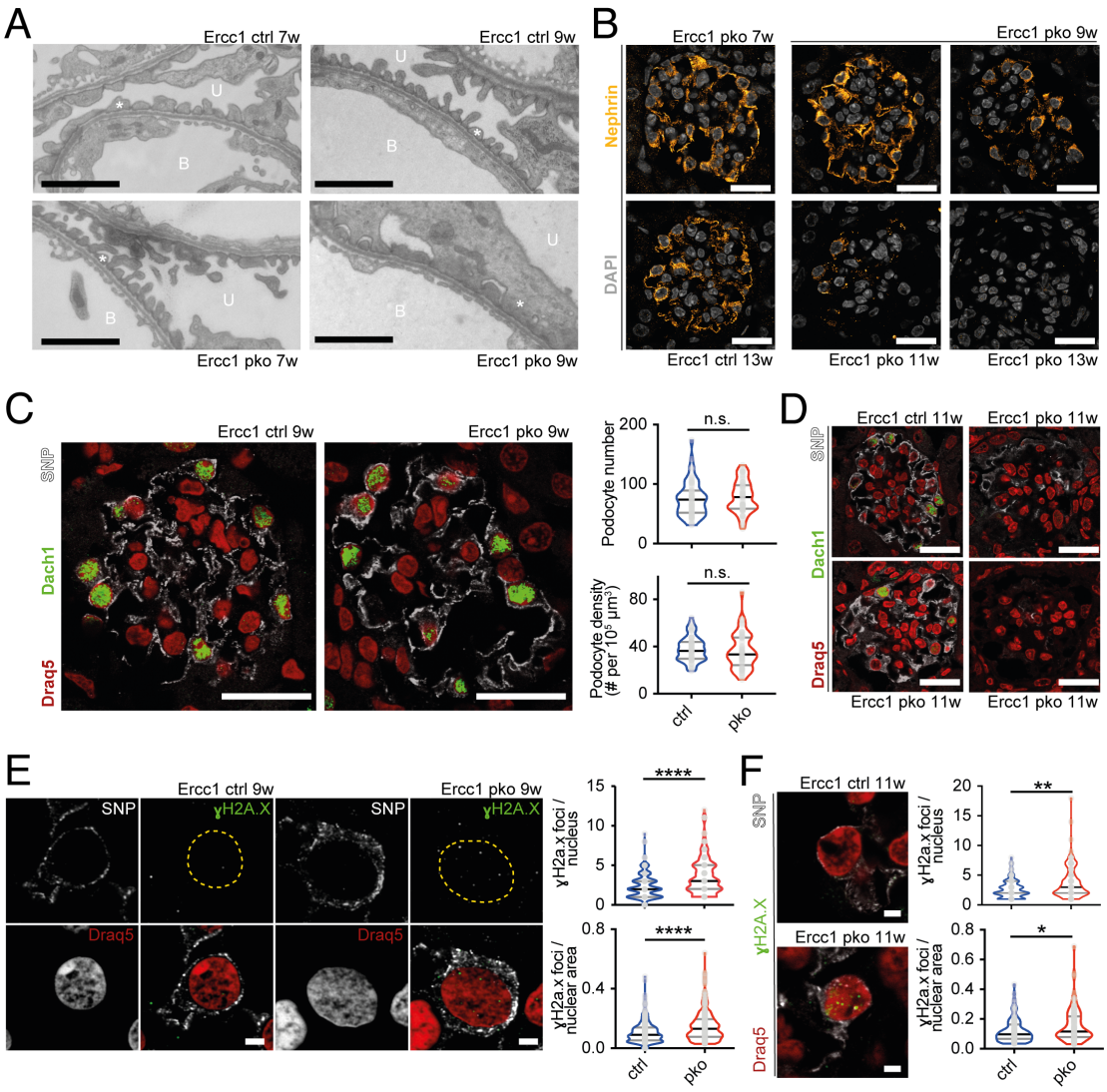

Figure 2: The podocyte-specific constitutive ko of *Ercc1* leads to foot process effacement and podocyte loss accompanied by accumulation of DNA damage.

A: Representative electron microscopy image of 7- and 9-week-old *Ercc1* ctrl and pko slit diaphragms, scalebar indicating 2 μm, B: blood side – intracapillary space, U: urinary side – Bowman's space, asterisk indicating podocyte foot process (n=3).

B: Representative immunofluorescence staining of slit diaphragm protein nephrin (yellow) with nuclear marker DAPI (grey) of *Ercc1* ctrl at 13 weeks of age and pko kidneys at 7, 9, 11, and 13 weeks of age, scalebar indicating 2 μm (n=5).

C: Representative immunofluorescence staining of podocyte proteins synaptopodin (SNP, gray), Dachshund homolog 1 (Dach1, green) [42] and far-red fluorescent DNA dye Draq5 (red) as a nuclear marker in sections of 9-week-old *Ercc1* ctrl and pko kidneys, with quantification of podocyte number and density of *Ercc1* ctrl and pko kidneys, scalebar indicating 10 μm (n=5).

D: Corresponding staining of podocyte proteins synaptopodin (gray), Dachshund homolog 1 (Dach1, green) [42] and far-red fluorescent DNA dye Draq5 (red) as a nuclear marker in paraffin-embedded sections of 11-week-old *Ercc1* ctrl and pko kidneys, scalebar indicating 10 μm (n=5).

E: Representative immunofluorescence staining of synaptopodin (SNP, gray), DNA damage marker γH2A.X (green) and nuclear marker Draq5 (red) in sections of 9-week-old *Ercc1* ctrl and pko kidneys, with quantification of γH2A.X foci per podocyte nucleus and nuclear area of *Ercc1* ctrl and pko kidneys, scalebar indicating 2 μm, yellow dotted line indicating nuclear border, n=5, 10 glomeruli per sample, 5 podocytes per glomerulus.

F: Representative immunofluorescence staining of synaptopodin (SNP, gray), DNA damage marker γH2A.X (green) and nuclear marker Draq5 (red) in sections of 11-week-old *Ercc1* ctrl and pko kidneys, with quantification of γH2A.X foci per podocyte nucleus and nuclear area of *Ercc1* ctrl and pko kidneys, scalebar indicating 2 μm, n=5, 10 glomeruli per sample, 5 podocytes per glomerulus.

All violin plots indicate median (black) and upper and lower quartile (gray), *p ≤ 0,05, **p ≤ 0,01, ***p ≤ 0,001, ****p ≤ 0,0001.

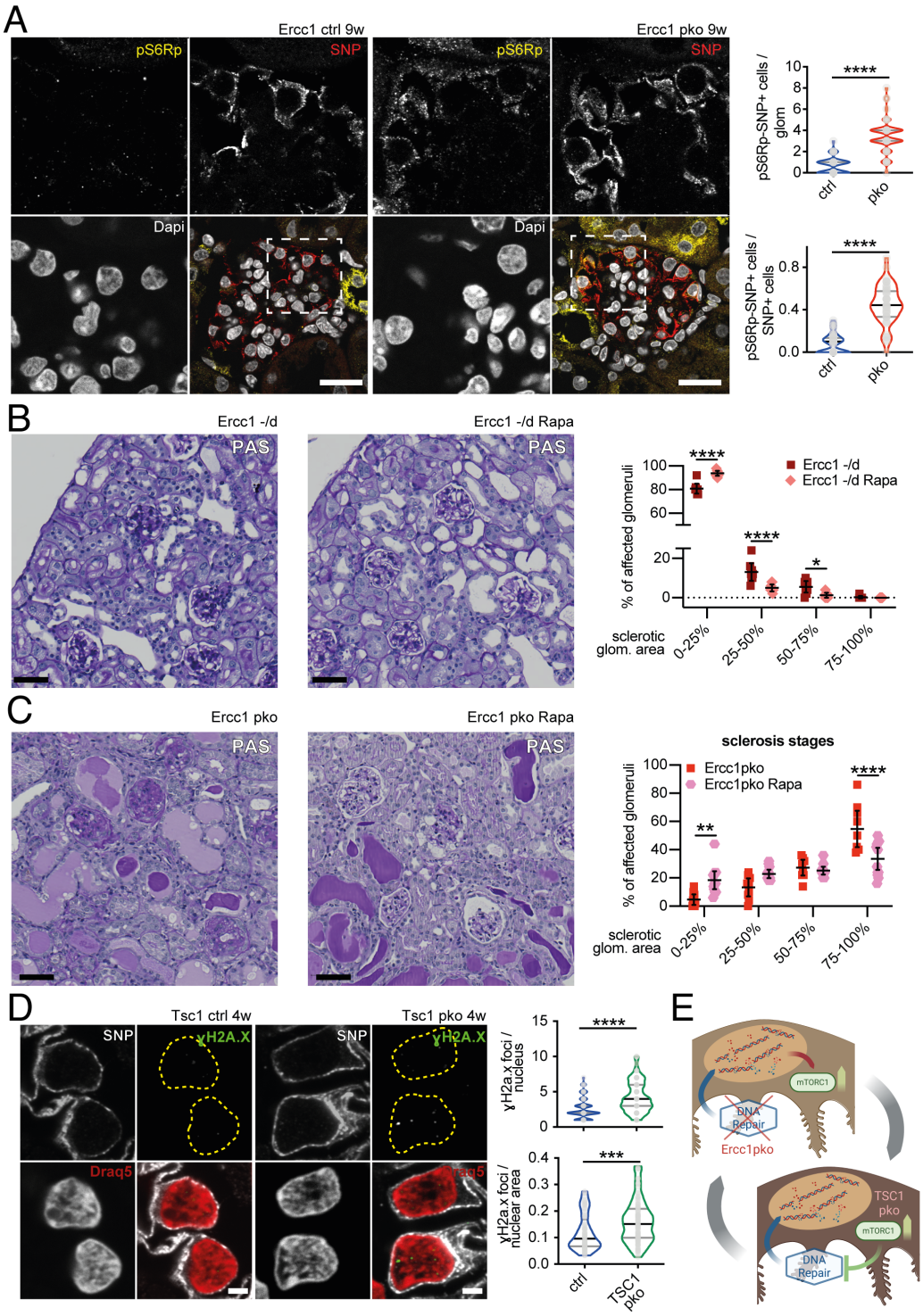

Figure 3: DNA damage leads to an activation of the mTORC1 pathway in podocytes *in vivo*.
A: Representative immunofluorescence staining of SNP, pS6RP and DAPI in sections of 9-week-old *Ercc1* ctrl and pko kidneys with quantification of SNP and pS6RP double positive cells per glomerulus and per total SNP positive cells, scalebar indicating 10 μm (n=5, 10 glomeruli per sample).
B: Representative Periodic Acid Schiff (PAS) staining of end-of-life *Ercc1* -/delta mice treated with 14 mg rapamycin per kg food from 8 weeks of age and quantification of sclerotic glomeruli (n = 8, 50 glomeruli per sample), scalebar indicating 50 μm.
C: Representative Periodic Acid Schiff (PAS) staining of *Ercc1* pko mice treated with vehicle (*Ercc1* pko) or rapamycin (*Ercc1* pko Rapa) from 6 weeks of age and quantification of sclerotic glomeruli, n ≥ 9, 50 glomeruli per sample, scalebar indicating 50 μm.
D: Representative immunofluorescence staining of synaptopodin (SNP, gray), DNA damage marker γH2A.X (green) and nuclear marker Draq5 (red) in sections of 4-week-old *Tsc1* ctrl and pko kidneys, with quantification of γH2A.X foci per podocyte nucleus and nuclear area of *Ercc1* ctrl and pko kidneys, yellow dotted line indicating nuclear border (n=5, 10 glomeruli per sample, 5 podocytes per glomerulus), scalebar indicating 2 μm.
E: Schematic overview depicting the potential interplay between defective DNA damage repair and increased mTORC1 signaling. In *Ercc1* pko mice, accumulation of DNA damage triggers mTORC1 signaling. In *Tsc1* pko mice, hyperactive mTORC1 signaling also leads to increased DNA damage foci.
All violin plots indicate median (black) and upper and lower quartile (gray), scatterplots indicate mean plus 95% confidence interval, *p ≤ 0,05, **p ≤ 0,01, ***p ≤ 0,001, ****p ≤ 0,0001.

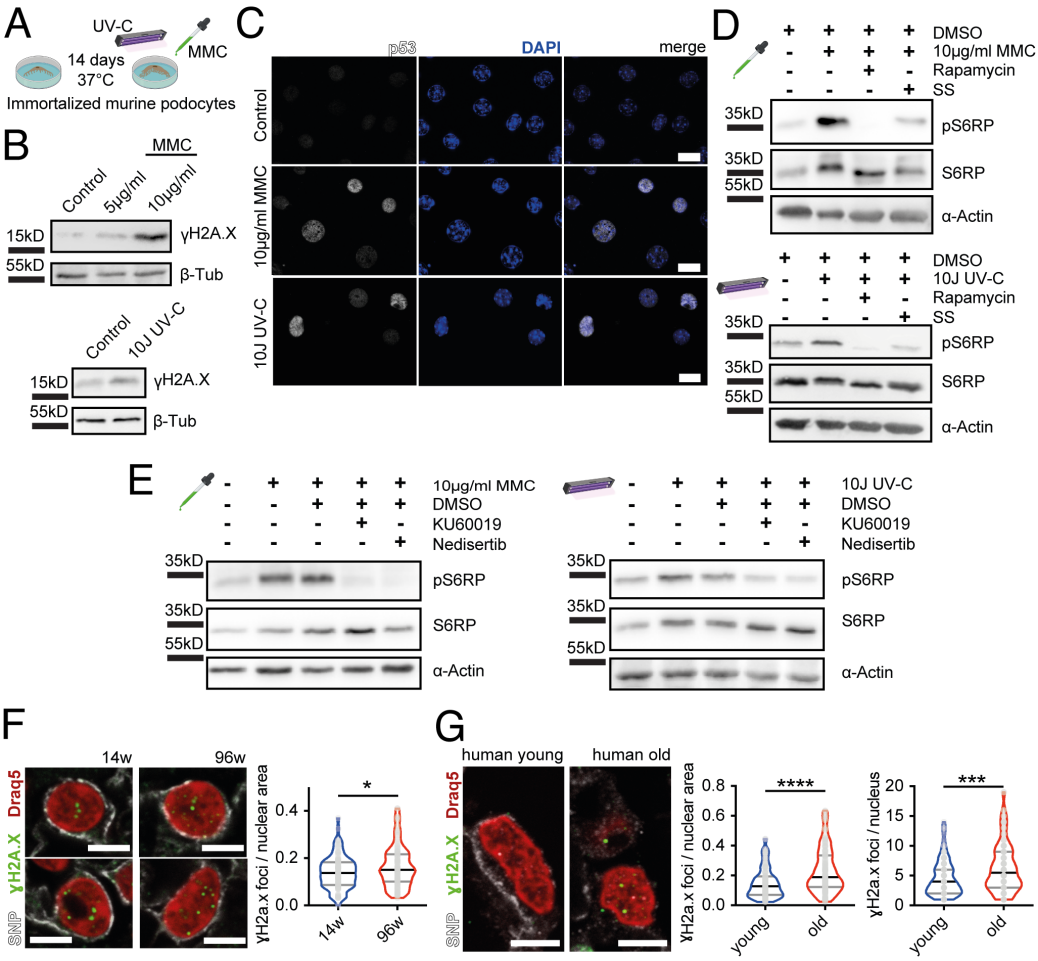

Figure 4: DNA damage leads to an activation of the mTORC1 pathway in podocytes *in vitro* through a DNA-PK-dependent mechanism and podocytes accumulate DNA damage with aging.

A: Schematic of *in vitro* protocol for the induction of DNA damage.

B: Representative immunoblot images for DNA damage marker γH2A.X and loading control protein beta-tubulin of immortalized murine podocyte lysates (n=3).

C: Representative immunofluorescence images for tumor suppressor p53 and nuclear marker DAPI in immortalized murine podocytes (n=3).

D: Representative immunoblot images for mTORC1 target phospho-S6 ribosomal protein (pS6RP), S6RP and loading control protein alpha-actin of immortalized murine podocyte lysates (n=3).

All cells imaged or lysed after treatment with mitomycin C (MMC) or ultraviolet C (UV-C) irradiation ± rapamycin or serum starvation (SS), n ≥ 4.

E: Representative immunoblot images for mTORC1 target phospho-S6 ribosomal protein (pS6RP), S6RP and loading control protein alpha-actin of immortalized murine podocyte lysates (n=3 MMC; n=6 UV-C).

All cells imaged or lysed after treatment with mitomycin C (MMC) or ultraviolet C (UV-C) irradiation ± ATM inhibitor KU60019 or DNA-PK inhibitor nedisertib.

F: Representative immunofluorescence staining of SNP, γH2A.X and Draq5 in sections of murine young and aged wildtype kidneys with quantification of γH2A.X foci per podocyte nucleus, scalebar indicating 2 μm, n=4, 5 glomeruli per sample, 5 podocytes per glomerulus.

G: Representative immunofluorescence staining of SNP, γH2A.X and Draq5 in sections of human young and old tumor nephrectomy kidneys with quantification of γH2A.X foci per podocyte nucleus, scalebar indicating 5 μm, n≥4, 5 glomeruli per sample, 5 podocytes per glomerulus.

All violin plots indicate median (black) and upper and lower quartile (gray), *p ≤ 0,05, ***p ≤ 0,001, ****p ≤ 0,0001.

897 **Supplementary Information:**

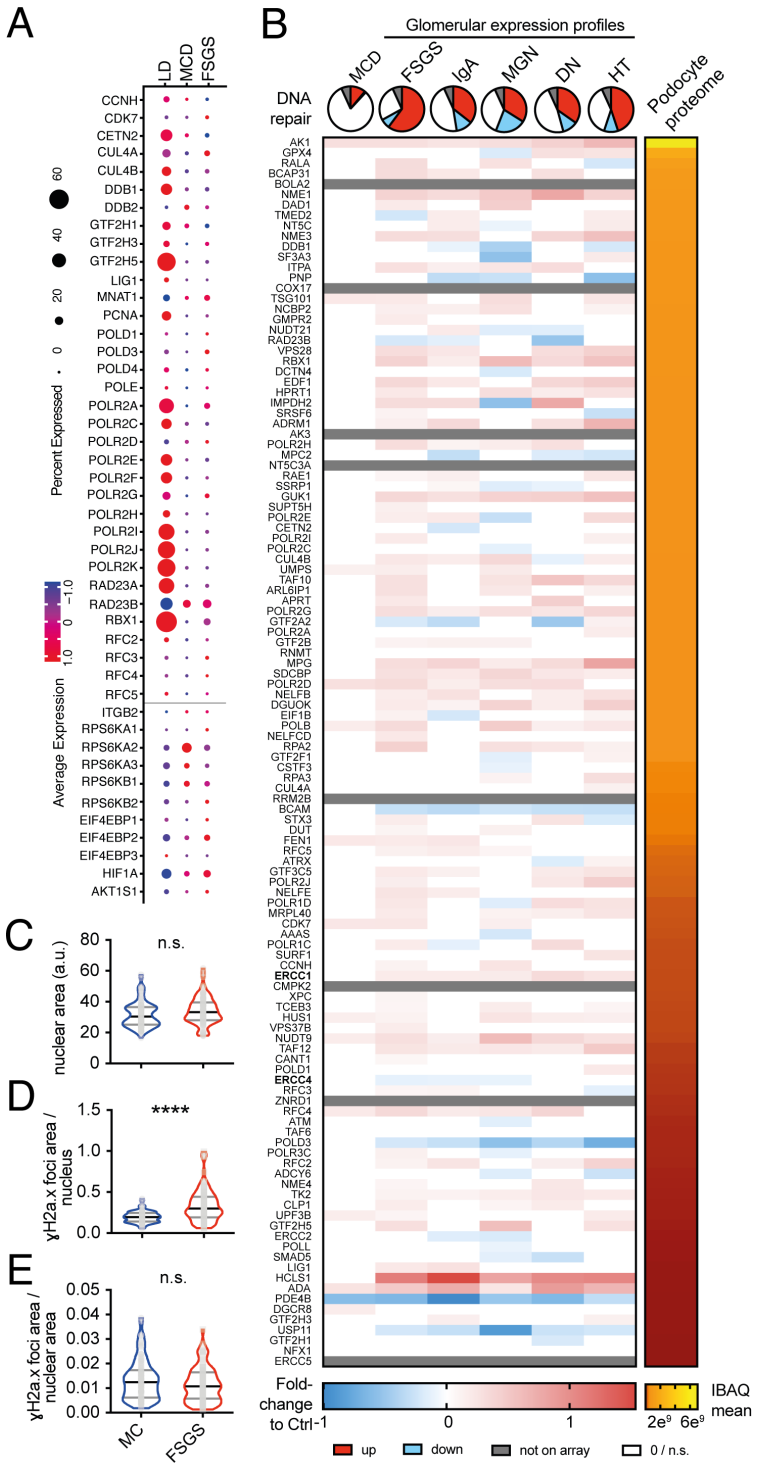

Figure S1:

A: Bubble plot indicating the differences in NER (excluding Ercc genes) and mTORC1 target gene expression in podocytes between living donor (LD) kidney samples, Minimal change disease (MCD) and FSGS biopsies obtained through single nucleus sequencing. Grey line indicating the split between NER and mTORC1 target genes.

B: Expression profile of 118 hallmark DNA repair genes in MCD, FSGS, IgA nephropathy (IgA), membranous nephropathy (MGN), diabetic nephropathy (DN), and hypertension (HT) glomeruli compared to controls depicted as parts of whole and single genes in heatmaps. Genes ranked by their protein abundance (Intensity-based absolute quantification - IBAQ) in murine podocyte proteome analysis[39].

C: Quantification of podocyte nuclear area of human MCD and FSGS biopsies (n=4, 4 glomeruli per sample, 5 podocytes per glomerulus).

D: Quantification of γH2A.X foci area per podocyte nucleus of human MCD and FSGS biopsies (n=4, 4 glomeruli per sample, 5 podocytes per glomerulus).

E: Quantification of γH2A.X foci area per podocyte nuclear area of human MCD and FSGS biopsies (n=4, 4 glomeruli per sample, 5 podocytes per glomerulus).

All violin plots indicate median (black) and upper and lower quartile (gray), ****$p \leq 0{,}0001$.

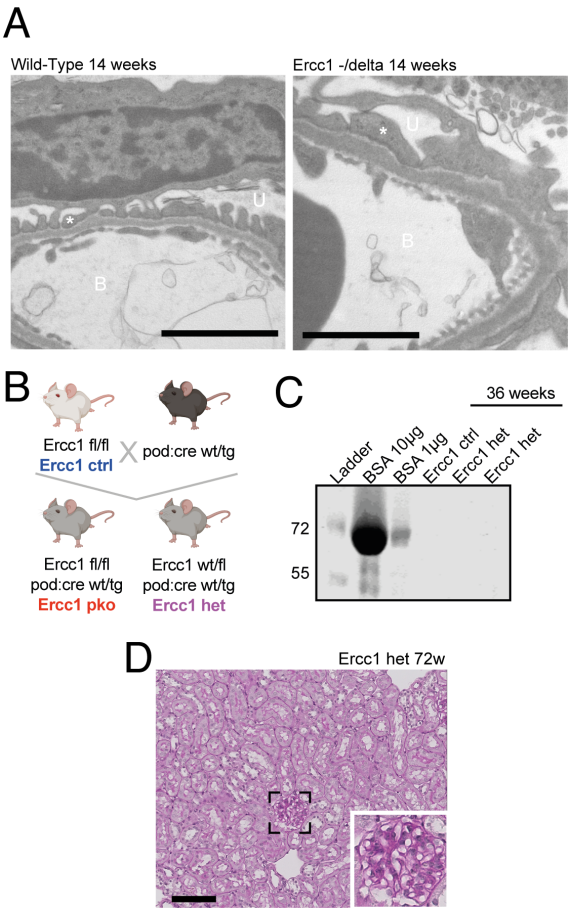

Fig S2:

A: Representative electron microscopy image of 14-week-old wild-type (WT) and *Ercc1* -/delta (Ercc1-/d) glomerular filtration barrier, scalebar indicating 2 μm, B: blood side – intracapillary space, U: urinary side – bowman's space, Asterisk indicating podocyte foot process (n=4).
B: Breeding scheme for homozygous and heterozygous podocyte-specific *Ercc1* pko mice.
C: Representative Coomassie blue staining of *Ercc1* ctrl and wt/pko (het) urine at 36 weeks of age; bovine serum albumin (BSA) was loaded as reference.
D: Representative Periodic Acid Schiff (PAS) staining of *Ercc1* wt/pko (het) kidney at 72 weeks of age, scalebar: 100 μm.

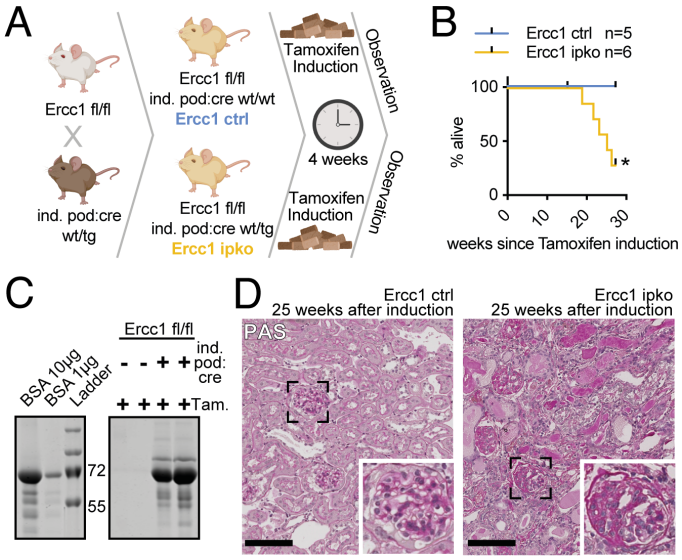

926 **Figure S3:**
927 A: Breeding and induction scheme for homozygous inducible podocyte-specific *Ercc1* ko mice (ipko).
928 B: Kaplan-Meyer curve depicting survival of *Ercc1* ctrl and ipko mice (Mantel-Cox test).
929 C: Representative Coomassie blue staining of *Ercc1* ctrl and ipko urine 18 weeks after induction with
930 tamoxifen; bovine serum albumin (BSA) was loaded as reference (n=6).
931 D: Representative Periodic Acid Schiff (PAS) staining of *Ercc1* ctrl and ipko mice 25 weeks after induction
932 with tamoxifen (n=6).
933 *p ≤ 0,05, scalebars: 100μm.

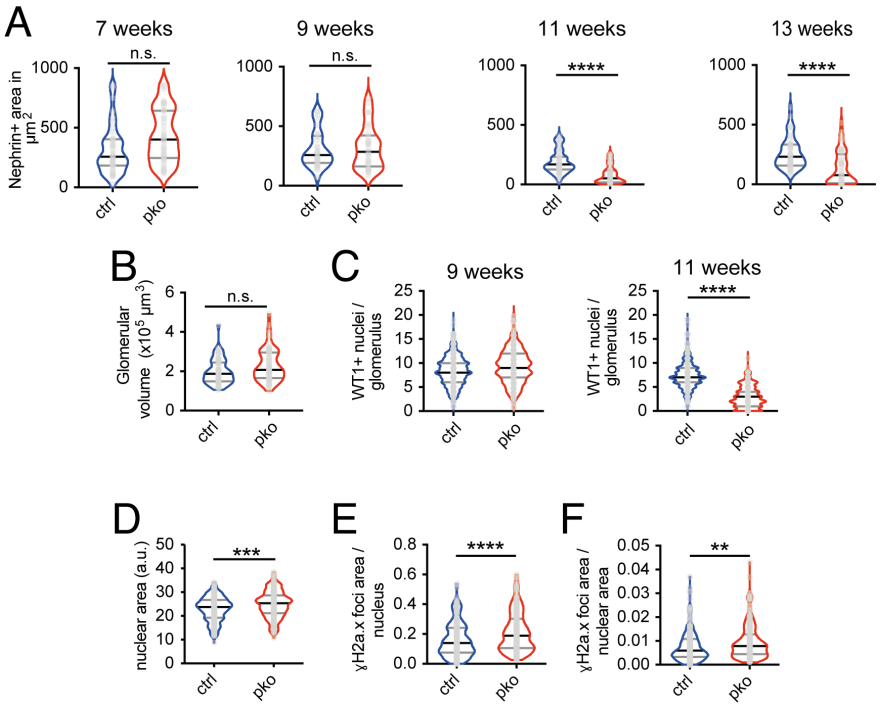

Figure S4:

A: Quantification of nephrin positive area in μm^2 of *Ercc1* ctrl and pko kidneys at 7, 9, 11, and 13 weeks of age, n=4, 10 glomeruli per sample.

B: Quantification of glomerular volume of 9-week-old *Ercc1* ctrl and pko kidneys, n = 5, 10 glomeruli per sample.

C: Quantification of WT+ nuclei per glomerulus of *Ercc1* ctrl and pko kidneys at 9 and 11 weeks of age, n = 4, ≥50 glomeruli per group

D: Quantification of podocyte nuclear are of 9-week-old *Ercc1* ctrl and pko kidneys, n = 5, 10 glomeruli per sample, 5 podocytes per glomerulus.

E: Quantification of γH2A.X foci area per podocyte nucleus of 9-week-old *Ercc1* ctrl and pko kidneys, n = 5, 10 glomeruli per sample, 5 podocytes per glomerulus.

F: Quantification of γH2A.X foci area per podocyte nuclear area of 9-week-old *Ercc1* ctrl and pko kidneys, n = 5, 10 glomeruli per sample, 5 podocytes per glomerulus.

All violin plots indicate median (black) and upper and lower quartile (gray), **p ≤ 0,01, ***p ≤ 0,001, ****p ≤ 0,0001.

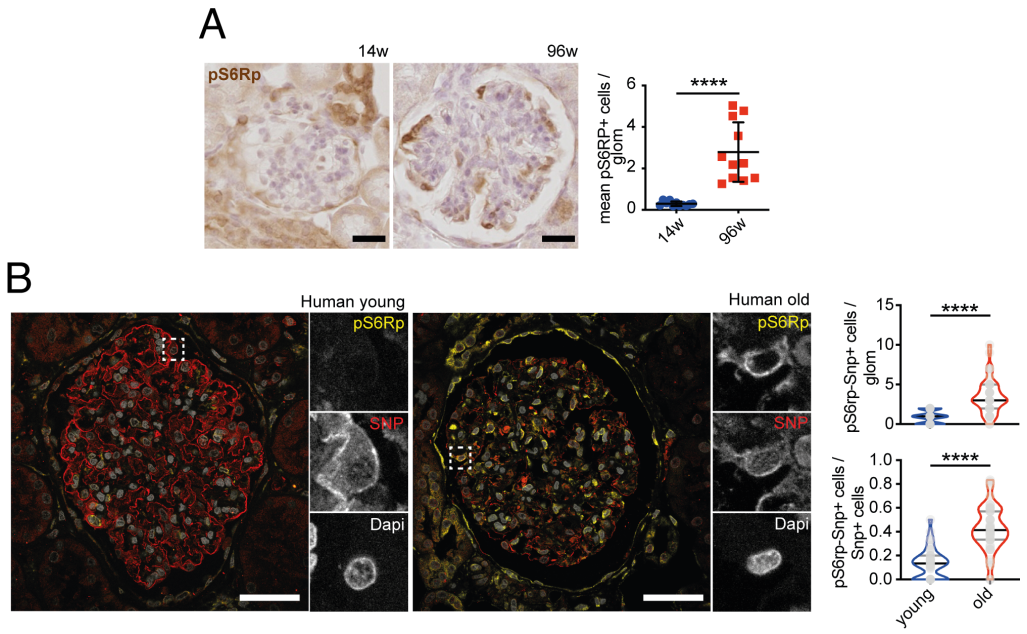

Figure S5:
A: Representative immunohistochemistry staining of pS6RP in sections of murine young and aged wildtype kidneys with quantification of pS6RP-positive cells per glomerulus, scalebar indicating 25 μm, n =11, 50 glomeruli per sample.
B: Representative immunofluorescence staining of SNP, pS6RP and DAPI in sections of young and old human tumor nephrectomy kidneys with quantification of SNP and pS6RP double positive cells per glomerulus and per total SNP positive cells, scalebar indicating 10 μm, n=≥4, 10 glomeruli per sample.
Scatterplot depicting mean and 95% confidence interval, all violin plots indicating median (black) and upper and lower quartile (gray), ****p ≤ 0,0001.

Table S1: Gene expression analysis of ERCB for Hallmark DNA Repair and Nucleotide Excision Repair Genes

Table S2: Clinical characteristics of FSGS patients

Table S3: eQTL analysis of DNA repair genes in FSGS patients
Ensg: ensemble gene ID; FDR: false discovery rate, PIP: posterior inclusion probability, AF: allele frequency, beta: expression difference to reference allele

Table S4: Full eQTL analysis of DNA repair genes in FSGS patients